

# High order relaxation schemes for non linear degenerate diffusion problems

Fausto Cavalli<sup>†§</sup>      Giovanni Naldi <sup>†§</sup>      Gabriella Puppo<sup>‡§</sup>  
 Matteo Semplice<sup>†§</sup>

March 29, 2022

## Abstract

Several relaxation approximations to partial differential equations have been recently proposed. Examples include conservation laws, Hamilton-Jacobi equations, convection-diffusion problems, gas dynamics problems. The present paper focuses onto diffusive relaxation schemes for the numerical approximation of nonlinear parabolic equations. These schemes are based on a suitable semilinear hyperbolic system with relaxation terms. High order methods are obtained by coupling ENO and WENO schemes for space discretization with IMEX schemes for time integration. Error estimates and convergence analysis are developed for semidiscrete schemes with numerical analysis for fully discrete relaxed schemes. Various numerical results in one and two dimensions illustrate the high accuracy and good properties of the proposed numerical schemes, also in the degenerate case. These schemes can be easily implemented on parallel computers and applied to more general systems of nonlinear parabolic equations in two- and three-dimensional cases.

## 1 Introduction

Relaxation approximations to nonlinear partial differential equations have been introduced [1, 2, 21, 23, 25, 27, 28] on the basis of the replacement of the equations with a suitable semilinear hyperbolic system with stiff relaxation terms. The idea can be explained by considering the case of a scalar conservation law

$$\frac{\partial u}{\partial t} + \frac{\partial f(u)}{\partial x} = 0,$$

---

<sup>†</sup>Dipartimento di Matematica, Università di Milano, Via Saldini 50, I-20100 Milano, Italy.

<sup>‡</sup>Dipartimento di Matematica, Politecnico di Torino, Corso Duca degli Abruzzi 24, 10129 Torino, Italy. [gabriella.puppo@polito.it](mailto:gabriella.puppo@polito.it)

<sup>§</sup>This work was partially supported by the MIUR/PRIN2005 project “Modellistica numerica per il calcolo scientifico ed applicazioni avanzate”.

for which Jin and Xin proposed in [23] the following relaxation approximation

$$\begin{cases} \frac{\partial u}{\partial t} + \frac{\partial v}{\partial x} = 0 \\ \frac{\partial v}{\partial t} + a \frac{\partial u}{\partial x} = -\frac{1}{\epsilon} (v - f(u)) \end{cases}$$

where  $\epsilon$  (relaxation time) is a small positive parameter and  $a$  is a positive constant satisfying

$$-\sqrt{a} \leq f'(u) \leq \sqrt{a}$$

for all  $u$ . For small values of  $\epsilon$  the previous system gives the following first order approximation of the original conservation law

$$\frac{\partial u}{\partial t} + \frac{\partial f(u)}{\partial x} = \epsilon \frac{\partial}{\partial x} \left( (a - f'(u)^2) \frac{\partial u}{\partial x} \right).$$

The generalization of the above model to multidimensional systems of conservation laws can be done in a natural way by adding more rate equations. One would expect that appropriate numerical schemes for the relaxation system yield accurate numerical approximations to the original equation or system when the relaxation rate  $\epsilon$  is sufficiently small. Numerically, the main advantage of solving the relaxation model over the original conservation law lies in the simple linear structure of characteristic fields and the localized lower order term. In particular, the semilinear nature of the relaxation system gives a new way to develop numerical schemes that are simple, general and Riemann solver free [18, 20, 23]. Several other relaxation approximation have been introduced recently. For example we mentioned here the work of Coquel and Perthame [10] for real gas computation, the relaxation schemes of Jin et al. [19] for curvature-dependent front propagation, the relaxation approximation in the rapid granular flow [22], the relaxation approximation and relaxation schemes for diffusion and convection-diffusion problems [21, 25, 27, 28]. Moreover, there are strong and interesting links between the relaxation approximation and the kinetic approach to nonlinear transport equations, based upon analogies with the passage from the Boltzmann equation to fluid mechanics (see for example [1, 2, 7]).

The aim of this work is to analyze from both a theoretical and computational point of view relaxation schemes that approximate the following nonlinear degenerate parabolic problem

$$\frac{\partial u}{\partial t} = D \Delta(p(u)), \quad x \in \mathbb{R}^d, \quad t > 0, \quad (1)$$

with initial data  $u(x, 0) = u_0(x) \in L^1(\mathbb{R}^d)$  and  $D > 0$  is a diffusivity coefficient. As usual, we will assume  $p : \mathbb{R} \rightarrow \mathbb{R}$  to be non-decreasing and Lipschitz continuous [35]. The equation is degenerate if  $p(0) = 0$ . We will also consider the same parabolic problem in a bounded domain  $\Omega \subset \mathbb{R}^d$  with Neumann boundary conditions. In the case  $p(u) = u^m$ ,  $m > 1$  the previous equation is the *porous media equation* which describes the flow of a gas through a porous interface according

to some constitutive relation like Darcy's law in order to link the velocity of the gas and its pressure. In this case the diffusion coefficient  $mu^{m-1}$  vanishes at the points where  $u \equiv 0$  and the governing parabolic equation degenerates there. The set of such points is called interface. Moreover the porous media equation can exhibit a finite speed of propagation for compactly supported initial data [3]. The influence of the degenerate diffusion terms make the dynamics of the interfaces difficult to study from both the theoretical and the numerical point of view. Another interesting case corresponds to  $0 < m < 1$  and it is referred to as the *fast diffusion equation* which appears, for example, in curvature-driven evolution and avalanches in sandpiles. In general the numerical analysis of equation (1) is difficult for at least two reasons: the appearance of singularities for compactly supported solutions and the growth of the size of the support as time increases (*retention property*).

From the numerical viewpoint, an usual technique to approximate (1) involves implicit discretization in time: it requires, at each time step, the discretization of a nonlinear elliptic problem. However, when dealing with nonlinear problems one generally tries to linearize them in order to take advantage of efficient linear solvers. Linear approximation schemes based on the so-called nonlinear Chernoff's formula with a suitable relaxation parameter have been studied for example in [6, 29, 30, 26] where also some energy error estimates have been investigated. Other linear approximation schemes have been introduced by Jäger, Kačur and Handlovičová [17, 24]. More recently, different approaches based on kinetic schemes for degenerate parabolic systems have been considered and analyzed by Aregba-Driollet, Natalini and Tang in [2]. Other approaches were investigated in the work of Karlsen et al. [13] based on a suitable splitting technique with applications to more general hyperbolic-parabolic convection-diffusion equations. Finally, a new scheme based on the maximum principle and on a perturbation and regularization approach was proposed by Pop and Yong in [32].

Our approach is inspired by relaxation schemes where the nonlinearity inside the equation is replaced by a semilinearity. This reduction is carried out in order to obtain numerical schemes that are easy to implement, also for parallel computing, even in the multidimensional case and for more general and complex problems, like oil recovery problems [12]. Moreover with our approach it is possible to improve numerical schemes by using high order methods and, in principle, different numerical approaches (finite volume, finite differences, ...). In particular, in this paper, in order to obtain high order methods, we couple ENO and WENO schemes for space discretization and IMEX schemes for time advancement. High order schemes may not reach their order of convergence due to the loss of regularity of the solution during the evolution. However they are interesting nevertheless for error reduction when the number of grid points is fixed or until discontinuities develop (both cases arise for example in nonlinear filtering in image analysis [36]).

The paper is organized as follows. Section 2 is devoted to the introduction of our relaxation schemes. The stability and error estimates of the semidiscrete scheme is provided in Section 3. In Section 4 we consider the fully discrete

relaxed scheme with nonlinear stability analysis, the numerical treatment of boundary conditions and the extension to the multi-dimensional case. Finally, the implementation of the method as well as the results of several numerical experiments are discussed in section 5.

## 2 Relaxation approximation of nonlinear diffusion

The main purpose of this work is to approximate solutions of a nonlinear, possibly degenerate, parabolic equation of the form (1). This framework is so general that it includes the porous medium equation  $p(u) = u^m$  with  $m > 1$  ([35] and references therein), non linear image processing [36], as well as a wide class of mildly nonlinear parabolic equations [14].

The schemes proposed in the present work are based on the same idea at the basis of the well-known relaxation schemes for hyperbolic conservation laws [23]. In the case of the nonlinear diffusion operator, an additional variable  $\vec{v}(x, t) \in \mathbb{R}^d$  and a positive parameter  $\varepsilon$  are introduced and the following relaxation system is obtained:

$$\begin{cases} \frac{\partial u}{\partial t} + \operatorname{div}(\vec{v}) = 0 \\ \frac{\partial \vec{v}}{\partial t} + \frac{D}{\varepsilon} \nabla p(u) = -\frac{1}{\varepsilon} \vec{v} \end{cases} \quad (1)$$

Formally, in the small relaxation limit,  $\varepsilon \rightarrow 0^+$ , system (1) approximates to leading order equation (1). In order to have bounded characteristic velocities and to avoid a singular differential operator as  $\varepsilon \rightarrow 0^+$ , a suitable parameter  $\varphi$  is introduced and (1) can be rewritten as:

$$\begin{cases} \frac{\partial u}{\partial t} + \operatorname{div}(\vec{v}) = 0 \\ \frac{\partial \vec{v}}{\partial t} + \varphi^2 \nabla p(u) = -\frac{1}{\varepsilon} \vec{v} + \left( \varphi^2 - \frac{D}{\varepsilon} \right) \nabla p(u) \end{cases} \quad (2)$$

Finally we remove the non linear term from the convective part, as in standard relaxation schemes, introducing a variable  $w(x, t) \in \mathbb{R}$  and rewriting the system as:

$$\begin{cases} \frac{\partial u}{\partial t} + \operatorname{div}(\vec{v}) = 0 \\ \frac{\partial \vec{v}}{\partial t} + \varphi^2 \nabla w = -\frac{1}{\varepsilon} \vec{v} + \left( \varphi^2 - \frac{D}{\varepsilon} \right) \nabla w \\ \frac{\partial w}{\partial t} + \operatorname{div}(\vec{v}) = -\frac{1}{\varepsilon} (w - p(u)) \end{cases} \quad (3)$$

Formally, as  $\varepsilon \rightarrow 0^+$ ,  $w \rightarrow p(u)$ ,  $\vec{v} \rightarrow -\nabla p(u)$  and the original equation is recovered.

In the previous system the parameter  $\varepsilon$  has physical dimensions of time and represents the so-called relaxation time. Furthermore,  $w$  has the same dimensions as  $u$ , while each component of  $\vec{v}$  has the dimension of  $u$  times a velocity; finally  $\varphi$  is a velocity. The inverse of  $\varepsilon$  gives the rate at which  $v$  decays onto  $-\nabla p(u)$  in the evolution of the variable  $\vec{v}$  governed by the stiff second equation of (3).

Equations (3) form a semilinear hyperbolic system with a stiff source term. The characteristic velocities of the hyperbolic part are given by  $0, \pm\varphi$ . The parameter  $\varphi$  allows to move the stiff terms  $\frac{D}{\varepsilon}\nabla p(u)$  to the right hand side, without losing the hyperbolicity of the system.

We point out that degenerate parabolic equations often model physical situations with free boundaries or discontinuities: we expect that schemes for hyperbolic systems will be able to reproduce faithfully these details of the solution. One of the main properties of (3) consists in the semilinearity of the system, that is all the nonlinearities are in the (stiff) source terms, while the differential operator is linear. Hence, the solution of the convective part requires neither Riemann solvers nor the computation of the characteristic structure at each time step, since the eigenstructure of the system is constant in time. Moreover, the relaxation approximation does not exploit the form of the nonlinear function  $p$  and hence it gives rise to a numerical scheme that, to a large extent, is independent of it, resulting in a very versatile tool.

We also anticipate here that, in the relaxed case (i.e.  $\varepsilon = 0$ ), the stiff source terms can be integrated solving a system that is already in triangular form and then it does not require iterative solvers.

### 3 The semidiscrete scheme

System (3) can be written in the form:

$$z_t + \operatorname{div} f(z) = \frac{1}{\varepsilon} g(z), \quad (1)$$

where

$$z = \begin{pmatrix} u \\ v \\ w \end{pmatrix} \quad f(z) = \begin{bmatrix} v^T \\ \Phi^2 w \\ v^T \end{bmatrix} \quad g(z) = \begin{pmatrix} 0 \\ -v + (\varphi^2 \varepsilon - D)\nabla w \\ p(u) - w \end{pmatrix} \quad (2)$$

and  $\Phi^2$  is the  $d \times d$  identity matrix times the scalar  $\varphi^2$ . We start discretizing the system in time using, for simplicity, a uniform time step  $\Delta t$ . Let  $z^n(x) = z(x, t^n)$ , with  $t^n = n\Delta t$ . Since equation (1) involves both stiff and non-stiff terms, it is a natural idea to employ different time-discretization strategies for each of them, as in [4, 31]. In this work we integrate (1) with a Runge-Kutta IMEX scheme [31], obtaining the following semidiscrete formulation

$$z^{n+1} = z^n - \Delta t \sum_{i=1}^{\nu} \tilde{b}_i \operatorname{div} f(z^{(i)}) + \frac{\Delta t}{\varepsilon} \sum_{i=1}^{\nu} b_i g(z^{(i)}), \quad (3)$$

where the  $z^{(i)}$ 's are the stage values of the Runge-Kutta scheme which are given by

$$z^{(i)} = z^n - \Delta t \sum_{k=1}^{i-1} \tilde{a}_{i,k} \operatorname{div} f(z^{(k)}) + \frac{\Delta t}{\varepsilon} \sum_{k=1}^i a_{i,k} g(z^{(k)}), \quad (4)$$

where  $\tilde{b}_i$ ,  $\tilde{a}_{ij}$  and  $b_i$ ,  $a_{ij}$  denote the coefficients of the explicit and implicit RK schemes, respectively. We assume that the implicit scheme is of diagonally implicit type. To find the  $z^{(i)}$ 's it is necessary in principle to solve a non linear system of equations which however can be easily decoupled. The system for the first stage  $z^{(1)}$  at time  $t^n$  is:

$$\begin{pmatrix} u^{(1)} \\ v^{(1)} \\ w^{(1)} \end{pmatrix} = \begin{pmatrix} u^n \\ v^n \\ w^n \end{pmatrix} + \frac{\Delta t}{\varepsilon} a_{11} \begin{pmatrix} 0 \\ -v^{(1)} + (\varphi^2 \varepsilon - D) \nabla w^{(1)} \\ p(u^{(1)}) - w^{(1)} \end{pmatrix}. \quad (5)$$

The first equation yields  $u^{(1)} = u^n$ , substituting in the third equation we immediately find  $w^{(1)}$  and finally, substituting  $w^{(1)}$  in the second equation, we compute  $v^{(1)}$ . In other words the system can be written in triangular form. For the following stage values, grouping the already computed terms in the vector  $B^{(i)}$  given by

$$B^{(i)} = z^n - \Delta t \sum_{k=1}^{i-1} \tilde{a}_{i,k} \operatorname{div} f(z^{(k)}) + \frac{\Delta t}{\varepsilon} \sum_{k=1}^{i-1} a_{i,k} g(z^{(k)}), \quad (6)$$

then the new stage values are given by

$$\begin{pmatrix} u^{(i)} \\ v^{(i)} \\ w^{(i)} \end{pmatrix} = B^{(i)} + \frac{\Delta t}{\varepsilon} a_{ii} \begin{pmatrix} 0 \\ -v^{(i)} + (\varphi^2 \varepsilon - D) \nabla w^{(i)} \\ p(u^{(i)}) - w^{(i)} \end{pmatrix}, \quad (7)$$

which is again a triangular system. In the numerical tests, we will apply IMEX schemes of order 1, 2 and 3.

Following [23] we set  $\varepsilon = 0$  thus obtaining the so called *relaxed scheme*. The computation of the first stage reduces to

$$\begin{aligned} u^{(1)} &= u^n \\ w^{(1)} &= p(u^{(1)}) \\ v^{(1)} &= -D \nabla w^{(1)} \end{aligned} \quad (8)$$

For the following stages the first equation is

$$u^{(i)} = u^n - \Delta t \sum_{k=1}^{i-1} \tilde{a}_{i,k} \operatorname{div} v^{(k)}. \quad (9)$$

In the other equations the convective terms are dominated by the source terms and thus  $v^{(i)}$  and  $w^{(i)}$  are given by

$$\begin{aligned} v^{(i)} &= -D \nabla w^{(i)}, \\ w^{(i)} &= p(u^{(i)}). \end{aligned} \quad (10)$$

We see that only the explicit part of the Runge-Kutta method is involved in the updating of the solution. Then, in the relaxed schemes we use only the explicit part of the tableaux. In particular we consider second and third order SSRK schemes [15], namely

IMEX1 (1<sup>st</sup> order)

$$\begin{array}{c|c} & 0 \\ \hline & 1 \end{array}$$

IMEX2 (2<sup>nd</sup> order)

$$\begin{array}{c|cc} & 0 & 0 \\ \hline & 1 & 0 \\ \hline & \frac{1}{2} & \frac{1}{2} \end{array}$$

IMEX3 (3<sup>rd</sup> order)

$$\begin{array}{c|ccc} & 0 & 0 & 0 \\ \hline & 1 & 0 & 0 \\ \hline & \frac{1}{4} & \frac{1}{4} & 0 \\ \hline & \frac{1}{6} & \frac{1}{6} & \frac{2}{3} \end{array}$$

### 3.1 Convergence of the semidiscrete relaxed scheme

The aim of this section is to show the  $L^1$  convergence of the solution of the semidiscrete in time relaxed scheme defined by equations (8),(9) and (10). We will extend the theorem proved in [6], where only the case of forward Euler timestepping was considered. In this section, for the sake of simplicity, we set  $D = 1$ .

Eliminating  $v$  from (8) and (9) using (10), we rewrite the relaxed scheme as

$$\begin{aligned} u^{(1)} &= u^n \\ w^{(1)} &= p(u^n) \end{aligned} \tag{11}$$

for the first stage, and

$$\begin{aligned} u^{(i)} &= u^n + \Delta t \sum_{k=1}^{i-1} \tilde{a}_{i,k} \Delta w^{(k)} \\ w^{(i)} &= p(u^{(i)}), \end{aligned} \tag{12}$$

for subsequent stages. We recall that a Runge-Kutta scheme for the ordinary differential equation  $y' = R(y)$  can also be written in the form [15]

$$\begin{aligned} y^{(1)} &= y^n \\ y^{(i)} &= \sum_{k=1}^{i-1} \alpha_{ik} \left( y^{(k)} + \Delta t \frac{\beta_{ik}}{\alpha_{ik}} R(y^{(k)}) \right) \quad i = 2, \dots, \nu, \end{aligned} \tag{13}$$

where  $y^{n+1} = y^{(\nu)}$ . For consistency,  $\sum_{k=1}^{i-1} \alpha_{ik} = 1$  for every  $i = 1, \dots, \nu$ . Moreover we assumed that  $\alpha_{ik} \geq 0$ ,  $\beta_{ik} \geq 0$  and that  $\alpha_{ik} = 0$  implies  $\beta_{ik} = 0$ . Under these assumptions, each stage value  $y^{(i)}$  can be written as a convex combination of forward Euler steps. This remark allows us to study the convergence of the Runge-Kutta scheme in terms of the convergence of the explicit forward Euler scheme applied to the non-linear diffusion problem.

This latter was studied in [6] via a nonlinear semigroup argument. In the following we review the approach of [6] and next we extend the proof to the case of a  $\nu$ -stages explicit Runge-Kutta scheme.

### 3.1.1 The forward Euler case

We wish to solve the evolution equation

$$\frac{du}{dt} + Lp(u) = 0 \quad u(\cdot, t = 0) = u_0, \quad (14)$$

on the domain  $\Omega$ , where  $L = -\Delta$  and  $p : \mathbb{R} \rightarrow \mathbb{R}$  is a non decreasing locally Lipschitz function such that  $p(0) = 0$ . Under these hypotheses, the nonlinear operator  $Au = Lp(u)$  with domain  $D(A) = \{u \in L^1(\Omega) : p(u) \in D(L)\}$  is m-accretive in  $L^1(\Omega)$ , that is  $\forall \varphi \in L^1(\Omega)$  and  $\forall \lambda > 0$  there exists a unique solution  $u \in D(A)$  such that  $u + \lambda Lp(u) = \varphi$  and the application defined by  $\varphi \mapsto u$  is a contraction[11].

Moreover  $D(A)$  is dense in  $L^1(\Omega)$ , so it follows that

$$S_A(t)u_0 = \lim_{m \rightarrow \infty} \left( \mathbb{I} + \frac{t}{m} A \right)^{-m} u_0 \quad (15)$$

is a contraction semigroup on  $L^1(\Omega)$  and  $S_A(t)u_0$  is the generalized solution of (14) in the sense of Crandall-Liggett [11]. Let  $S(t)$  be the linear contraction semigroup generated by  $-L$ , that is  $u(t) = S(t)u_0$  is the solution of the initial value problem  $u_t = -L(u)$  and  $u(\cdot, t = 0) = u_0$ . The algorithm proposed in [6] is

$$\frac{u^{n+1} - u^n}{\tau} + \left[ \frac{\mathbb{I} - S(\sigma_\tau)}{\sigma_\tau} \right] p(u^n) = 0, \quad (16)$$

where  $\tau$  is the timestep and  $\sigma_\tau \downarrow 0$ . This can be written as

$$u^{n+1} = F_E(\tau)u^n \quad \text{where } F_E(\tau)\varphi = \varphi + \frac{\tau}{\sigma_\tau} [S(\sigma_\tau) - \mathbb{I}] p(\varphi). \quad (17)$$

Hence

$$u^n = (F_E(\tau))^n u_0. \quad (18)$$

The proof in [6] is based on the following argument. Note that formally  $S(\sigma_\tau)\varphi \sim e^{-\sigma_\tau L}\varphi$ . Let  $t = \tau n$

$$\begin{aligned} u(t) &= \left[ \mathbb{I} + \frac{t}{n\sigma_\tau} (S(\sigma_\tau) - \mathbb{I}) \circ p \right]^n u_0 \\ &= \left[ \mathbb{I} + \frac{t}{n\sigma_\tau} (e^{-\sigma_\tau L} - \mathbb{I}) \circ p \right]^n u_0 \quad \text{if } \sigma_\tau \rightarrow 0 \\ &= \left[ \mathbb{I} - \frac{t}{n} L \circ p \right]^n u_0 \\ &\rightarrow S_A(u_0) \quad \text{when } n \rightarrow \infty \end{aligned} \quad (19)$$

The convergence proof requires that  $\mu \frac{\tau}{\sigma_\tau} \leq 1$  where  $\mu$  is the Lipschitz constant of  $p(u)$ . We point out that  $\sigma_\tau$  is linked to the spatial approximation of the operator  $L$  and in our scheme this requirement is reflected in the stability condition of the fully discrete scheme (see Section 4)



### 3.1.2 Runge-Kutta schemes

Now we are going to describe the case of a  $\nu$ -stages Runge-Kutta scheme, proving its convergence.

Let  $t > 0$  and  $\tau = t/n$  with  $n \geq 1$ ; let  $\sigma_\tau : (0, \infty) \rightarrow (0, \infty)$  be a function such that  $\lim_{\tau \rightarrow 0} \sigma_\tau = 0$ .

$$\begin{aligned} u^{(1)} &= u^n, \\ u^{(i)} &= \sum_{k=1}^{i-1} \alpha_{ik} \left[ u^{(k)} + \tau \frac{\beta_{ik}}{\alpha_{ik}} A(u^{(k)}) \right] \quad i = 2, \dots, \nu \end{aligned} \quad (20)$$

and proceeding as in (19), this becomes

$$\begin{aligned} u^{(1)} &= u^n, \\ u^{(i)} &= \sum_{k=1}^{i-1} \alpha_{ik} \left[ u^{(k)} + \tau \frac{\beta_{ik}}{\alpha_{ik}} (S(\sigma_\tau) - \mathbb{I}) \circ p(u^{(k)}) \right] \quad i = 2, \dots, \nu \\ u^{n+1} &= u^{(\nu)} \end{aligned} \quad (21)$$

We now extend (17) to the Runge-Kutta scheme defined by equation (21). Define, for  $\phi \in L^1(\Omega)$ ,

$$\begin{aligned} F^{(1)}(\tau)\phi &= \phi, \\ F^{(i)}(\tau)\phi &= \sum_{k=1}^{i-1} \alpha_{ik} F^{(k)}(\tau)\phi + \frac{\tau \beta_{ik}}{\sigma_\tau} [S(\sigma_\tau) - \mathbb{I}] p(F^{(k)}(\tau)\phi), \\ F(\tau)\phi &= F^{(\nu)}(\tau)\phi \end{aligned} \quad (22)$$

and therefore

$$u^n(t) = [F(\tau)]^n u_0. \quad (23)$$

Let  $u(t)$  be the generalized solution of (14). The following theorem proves the convergence of the semidiscrete solution to  $u(t)$ .

**Theorem 1.** *Assume  $u^0 \in L^\infty(\Omega)$ , and  $\|u^0\|_\infty = M$ ; let  $p$  be a non-decreasing Lipschitz continuous function on  $[-M, M]$  with Lipschitz constant  $\mu$ . Assume that the following conditions hold*

$$\left\{ \begin{array}{l} \alpha_{ik} \geq 0, \\ \beta_{ik} \geq 0, \\ \alpha_{ik} = 0 \Rightarrow \beta_{ik} = 0, \\ \sum_{k=1}^{i-1} \alpha_{ik} = 1 \text{ (consistency),} \\ \frac{\mu\tau}{\sigma_\tau} \leq \min \frac{\alpha_{ik}}{\beta_{ik}}, \text{ for } \tau > 0, \alpha_{ik} \neq 0 \text{ (stability),} \end{array} \right. \quad (24)$$

then  $\lim_{n \rightarrow \infty} u^n(t) = u(t)$  in  $L^1$ . Moreover the convergence is uniform for  $t$  in any given bounded interval.

The proof follows the steps of [6]: first we show that  $u^n$  verifies a maximum principle (Lemma 1) and that  $F$  is a contraction (Lemma 2) and finally we apply the non linear Chernoff formula[8].

**Lemma 1.** *If (24) is verified, then  $-M \leq u^n \leq M \quad \forall n$ .*

*Proof.* We argue by induction on  $n$ : we assume that  $-M \leq u^n \leq M$  and we show that  $-M \leq u^{n+1} \leq M$ . Let

$$u^{(i)} = F^{(i)}(\tau)u^n \quad (25)$$

Since  $u^{n+1} = u^{(\nu)}$ , it suffices to prove that  $-M \leq u^{(i)} \leq M$  for  $i = 1, \dots, \nu$ . We prove this by induction on  $i$ . When  $i = 1$ , the statement is true thanks to the induction hypothesis on  $n$  and being  $F^{(1)} = \mathbb{I}$ . Let's assume that  $-M \leq u^{(i-1)} \leq M$  holds; we are going to show that

$$-M \leq u^{(i)} = F^{(i)}(\tau)u^n \leq M. \quad (26)$$

The function  $s \mapsto \alpha_{ik}s - \frac{\tau\beta_{ik}}{\sigma_\tau}p(s)$  is non decreasing thanks to (24) and the hypotheses on the function  $p$ . By the induction hypothesis on  $i$ , we have that for  $k = 1, \dots, i-1$

$$-\alpha_{ik}M - \frac{\tau\beta_{ik}}{\sigma_\tau}p(-M) \leq \alpha_{ik}u^{(k)} - \frac{\tau\beta_{ik}}{\sigma_\tau}p(u^{(k)}) \leq \alpha_{ik}M - \frac{\tau\beta_{ik}}{\sigma_\tau}p(M). \quad (27)$$

Using again the induction hypothesis on  $i$ , recalling that  $p$  is non-decreasing, since  $S$  is a contraction in  $L^\infty$  [6] and  $p(-M) \leq p(u^{(k)}) \leq p(M)$ ,

$$p(-M) \leq S\left(p(u^{(k)})\right) \leq p(M) \quad (28)$$

Multiplying the last equation by  $\frac{\tau\beta_{ik}}{\sigma_\tau}$  and summing it to equation (27), we get

$$-\alpha_{ik}M \leq \alpha_{ik}u^{(k)} + \frac{\tau\beta_{ik}}{\sigma_\tau}(S - \mathbb{I})p(u^{(k)}) \leq \alpha_{ik}M, \quad k = 1, \dots, i-1 \quad (29)$$

Summing for  $k = 1, \dots, i-1$  and using the consistency relation of (24):

$$-M \leq \sum_{k=1}^{i-1} \alpha_{ik}u^{(k)} + \frac{\tau\beta_{ik}}{\sigma_\tau}(S - \mathbb{I})p(u^{(k)}) \leq M \quad (30)$$

In particular this is valid when  $i = \nu$ , proving that  $-M \leq u^{(n+1)} \leq M$ .  $\square$

Now we can replace  $p$  by  $\bar{p}$ , where  $\bar{p} = p$  in  $-M \leq x \leq M$ ,  $\bar{p} = p(M)$  for  $x \geq M$  and  $\bar{p} = p(-M)$  for  $x \leq -M$ : the algorithm is the same and in what follows we can assume that  $p$  is Lipschitz continuous with constant  $\mu$  on all  $\mathbb{R}$ .

**Lemma 2.** *If the hypotheses of Theorem 1 hold, then  $F(\tau)$  is a contraction on  $L^1(\Omega)$ , i.e.*

$$\|F(\tau)\phi - F(\tau)\psi\|_1 \leq \|\phi - \psi\|_1 \quad \forall \psi, \phi \in L^1 \quad (31)$$

*Proof.* We start showing that the result holds for a single forward Euler step. Recalling the definition of  $F_E$  from (17)

$$\begin{aligned} \|F_E(\tau)\phi - F_E(\tau)\psi\|_1 &\leq \frac{\tau}{\sigma_\tau} \|S(\sigma_\tau)[p(\phi) - p(\psi)]\|_1 + \left\| \left( \phi - \psi \right) - \frac{\tau}{\sigma_\tau} [p(\phi) - p(\psi)] \right\|_1 \\ &\leq \frac{\tau}{\sigma_\tau} \|p(\phi) - p(\psi)\|_1 + \left\| \left( \phi - \frac{\tau}{\sigma_\tau} p(\phi) \right) - \left( \psi - \frac{\tau}{\sigma_\tau} p(\psi) \right) \right\|_1 \\ &= \|\phi - \psi\|_1 \end{aligned} \tag{32}$$

where we used the contractivity of  $S$ . The last equality relies on the fact that  $p$  and the function  $x \mapsto x - \frac{\tau}{\sigma_\tau} p(x)$  are non-decreasing, which in turn is guaranteed by the stability condition, that in this case reduces to  $\mu\tau/\sigma_\tau \leq 1$  [6].

In the general case we have:

$$\begin{aligned} \|F^{(i)}(\tau)\phi - F^{(i)}(\tau)\psi\|_1 &\leq \sum_{k=1}^{i-1} \alpha_{ik} \left\| F_E \left( \frac{\tau\beta_{ik}}{\alpha_{ik}} \right) F^{(k)}(\tau)\phi - F_E \left( \frac{\tau\beta_{ik}}{\alpha_{ik}} \right) F^{(k)}(\tau)\psi \right\|_1 \\ &\leq \sum_{k=1}^{i-1} \alpha_{ik} \|F^{(k)}(\tau)\phi - F^{(k)}(\tau)\psi\|_1 \\ &\leq \|\phi - \psi\|_1 \end{aligned} \tag{33}$$

In the second inequality we used the contractivity of  $F_E$  and the stability condition, while in the third one we apply an induction argument on the contractivity of  $F^{(k)}$ , the positivity constraint on  $\alpha_{ik}$  and  $\beta_{ik}$ , as well as the consistency condition  $\sum_k \alpha_{ik} = 1$ . Setting  $i = \nu$  yields the result.  $\square$

*Proof of Theorem 1.* Let  $\psi_\tau$  and  $\psi$  be respectively

$$\psi_\tau = \left( I + \frac{\lambda}{\tau} (I - F(\tau)) \right)^{-1} \phi \quad \text{and} \quad \psi = (I + \lambda A)^{-1} \phi. \tag{34}$$

The function  $\psi$  exists since the operator  $A$  is m-accretive, whereas the existence of the function  $\psi_\tau$  is guaranteed by the following fixed-point argument. Let

$$G(y) = \frac{1}{1+\eta} \phi + \frac{\eta}{\eta+1} F(\tau)y$$

where  $\phi \in L^1$ ,  $y \in \overline{D(A)}$  and  $\eta \geq 0$ . We have,

$$\|G(y) - G(x)\| = \frac{\eta}{\eta+1} \|F(\tau)y - F(\tau)x\| \leq \frac{\eta}{\eta+1} \|y - x\|$$

since  $F$  is a contraction, as proved in Lemma 2. Thus  $G$  is also a contraction and therefore it possesses a unique fixed point which coincides with  $\psi_\tau$ .

We want to show that

$$\psi_\tau \rightarrow \psi \quad \text{in } L^1$$

as  $\tau \rightarrow 0$  for each fixed  $\lambda > 0$ . Let

$$\phi_\tau = \psi + \frac{\lambda}{\tau} (\mathbb{I} - F(\tau))\psi.$$

We want to estimate  $\psi_\tau - \psi$  in terms of  $\phi_\tau - \phi$ .

$$\phi_\tau - \phi = \left( 1 + \frac{\lambda}{\tau} \right) (\psi - \psi_\tau) - \frac{\lambda}{\tau} (F(\tau)\psi - F(\tau)\psi_\tau)$$

Therefore

$$(1 + \frac{\lambda}{\tau})(\psi - \psi_\tau) - (\phi_\tau - \phi) = \frac{\lambda}{\tau}(F(\tau)\psi - F(\tau)\psi_\tau)$$

and taking norms and using the fact that  $F$  is contraction we have

$$\left| (1 + \frac{\lambda}{\tau})\|\psi - \psi_\tau\| - \|\phi_\tau - \phi\| \right| \leq \|(1 + \frac{\lambda}{\tau})(\psi - \psi_\tau) - (\phi_\tau - \phi)\| \leq \frac{\lambda}{\tau}\|\psi - \psi_\tau\|$$

In particular

$$(1 + \frac{\lambda}{\tau})\|\psi - \psi_\tau\| - \|\phi_\tau - \phi\| \leq \frac{\lambda}{\tau}\|\psi - \psi_\tau\|$$

and therefore  $\|\psi - \psi_\tau\| \leq \|\phi - \phi_\tau\|$ .

Now we estimate  $\|\phi - \phi_\tau\|$  in the simple case of a forward Euler scheme. Note that

$$\phi - \phi_\tau = \lambda A\psi - \frac{\lambda}{\tau}(\mathbb{I} - F(\tau))\psi$$

and thus  $\|\phi - \phi_\tau\|$  measures a sort of consistency error. For a single forward Euler step,  $F = F_E$  where  $F_E$  is defined in (17). Thus

$$\|\phi - \phi_\tau\| = \lambda \left\| A\psi - \frac{1}{\sigma_\tau}(\mathbb{I} - S(\sigma_\tau))p(\psi) \right\| \rightarrow 0 \quad (35)$$

as  $\tau \rightarrow 0$  since  $\frac{\mathbb{I} - S(\sigma_\tau)}{\sigma_\tau}p(\psi) \rightarrow Lp(\psi) = A\psi$ .

The more general case of a  $\nu$ -stages Runge-Kutta scheme can be carried out by induction following the procedure already applied in the proofs of the previous lemmas.

We now use Theorem 3.2 of [8] which, specialized to our case, can be written as follows. Assume that  $F(\tau) : L^1 \rightarrow L^1$  for  $\tau > 0$  is a family of contractions. Assume further that an  $m$ -accretive operator  $A$  is given and let  $S(t)$  be the semi-group generated by  $A$ . Assume further that the family  $F(\tau)$  and the operator  $A$  are linked by the following formula

$$\psi_\tau = \left( I + \frac{\lambda}{\tau}(I - F(\tau)) \right)^{-1} \phi \rightarrow \psi = (I + \lambda A)^{-1} \phi \quad (36)$$

for each  $\phi \in L^1$ . Then

$$\lim_{n \rightarrow \infty} F\left(\frac{t}{n}\right)^n \phi = S(t)\phi \quad \forall \phi \in L^1.$$

□

## 4 Fully discrete relaxed scheme

In order to complete the description of the scheme, we need to specify the space discretization. We will use discretizations based on finite differences, in order to avoid cell coupling due to the source terms.

Note that the IMEX technique reduces the integration to a cascade of relaxation and transport steps. The former are the implicit parts of (5) and (7), while the transport steps appear in the evaluation of the explicit terms  $B^{(i)}$  in (6). Since (5) and (7) involve only local operations, the main task of the space discretization is the evaluation of  $\text{div}(f)$ , where we will exploit the linearity of  $f$  in its arguments.

#### 4.1 One dimensional scheme

Let us introduce a uniform grid on  $[a, b] \subset \mathbb{R}$ ,  $x_j = a - \frac{b}{2} + jh$  for  $j = 1, \dots, n$ , where  $h = (b - a)/n$  is the grid spacing and  $n$  the number of cells. The fully discrete scheme may be written as

$$z_j^{n+1} = z_j^n - \Delta t \sum_{i=1}^{\nu} \tilde{b}_i \left( F_{j+1/2}^{(i)} - F_{j-1/2}^{(i)} \right) + \frac{\Delta t}{\varepsilon} \sum_{i=1}^{\nu} b_i g(z_j^{(i)}), \quad (1)$$

where  $F_{j+1/2}^{(i)}$  are the numerical fluxes, which are the only item that we still need to specify. For convergence it is necessary to write the scheme in conservation form. Thus, following [34], we introduce the function  $\hat{F}$  such that

$$f(z(x, t)) = \frac{1}{h} \int_{x-h/2}^{x+h/2} \hat{F}(s, t) ds \quad \Rightarrow \quad \frac{\partial f}{\partial x}(z(x_j, t)) = \frac{1}{h} \left( \hat{F}(x_{j+1/2}, t) - \hat{F}(x_{j-1/2}, t) \right).$$

The numerical flux function  $F_{j+1/2}$  approximates  $\hat{F}(x_{j+1/2})$ .

In order to compute the numerical fluxes, for each stage value, we reconstruct boundary extrapolated data  $z_{j+1/2}^{(i)\pm}$  with a non-oscillatory interpolation method from the point values  $z_j^{(i)}$  of the variables at the center of the cells. Next we apply a monotone numerical flux to these boundary extrapolated data.

To minimize numerical viscosity we choose the Godunov flux, which in the present case of a linear system of equations reduces to the upwind flux. In order to select the upwind direction we write the system in characteristic form. The characteristic variables relative to the eigenvalues  $\varphi, -\varphi, 0$  (in one space dimension  $\varphi$  reduces to a scalar parameter) are respectively

$$U = \frac{v + \varphi w}{2\varphi} \quad V = \frac{\varphi w - v}{2\varphi} \quad W = u - w. \quad (2)$$

Note that  $u = U + V + W$ . Therefore the numerical flux in characteristic variables is  $F_{j+1/2} = (\varphi U_{j+1/2}^-, -\varphi V_{j+1/2}^+, 0)$ .

The accuracy of the scheme depends on the accuracy of the reconstruction of the boundary extrapolated data. For a first order scheme we use a piecewise constant reconstruction such that  $U_{j+1/2}^- = U_j$  and  $V_{j+1/2}^+ = V_{j+1}$ . For higher order schemes, we use ENO or WENO reconstructions of appropriate accuracy ([33]).

For  $\varepsilon \rightarrow 0$  we obtain the relaxed scheme. Recall from equation (10) that the relaxation steps reduce to

$$w_j^{(i)} = p(u_j^{(i)}), \quad v_j^{(i)} = -D\widehat{\nabla} w_j^{(i)}, \quad (3)$$

where  $\widehat{\nabla}$  is a suitable approximation of the one-dimensional gradient operator. Thus the transport steps need to be applied only to  $u^{(i)}$

$$u_j^{(i)} = u_j^n - \lambda \sum_{k=1}^{i-1} \tilde{a}_{i,k} \left[ \varphi \left( U_{j+1/2}^{(k)-} - U_{j-1/2}^{(k)-} \right) - \varphi \left( V_{j+1/2}^{(k)+} - V_{j-1/2}^{(k)+} \right) \right] \quad (4)$$

Finally, taking the last stage value and going back to conservative variables,

$$u_j^{n+1} = u_j^n - \frac{\lambda}{2} \sum_{i=1}^{\nu} \tilde{b}_i \left( [v_{j+1/2}^{(i)-} + v_{j+1/2}^{(i)+} - (v_{j-1/2}^{(i)-} + v_{j-1/2}^{(i)+})] + \varphi [w_{j+1/2}^{(i)-} - w_{j+1/2}^{(i)+} - (w_{j-1/2}^{(i)-} - w_{j-1/2}^{(i)+})] \right) \quad (5)$$

We wish to emphasize that the scheme reduces to the time advancement of the single variable  $u$ . Although the scheme is based on a system of three equations, the construction is used only to select the correct upwinding for the fluxes of the relaxed scheme and the computational cost of each time step remains moderate.

## 4.2 Non linear stability for the first order scheme

The relaxed scheme in the first order case reduces to:

$$u_j^{n+1} = u_j^n + \frac{\lambda}{2} (\partial_x p(u^n)|_{j+1} - \partial_x p(u^n)|_{j-1}) + \frac{\lambda}{2} \varphi (p(u_{j+1}^n) - 2p(u_j^n) + p(u_{j-1}^n)) \quad (6)$$

We wish to compute the restrictions on  $\lambda$  and  $\varphi$  so that the scheme is total variation non-increasing. We select the centered finite difference formula to approximate the partial derivatives of  $p(u)$ ; we drop the index  $n$  and write  $p_j$  for  $p(u_j^n)$ . Define  $\Delta_{j+1/2} = \frac{p_{j+1} - p_j}{u_{j+1} - u_j}$  and observe that these quantities are always nonnegative since  $p$  is nondecreasing. We obtain

$$\begin{aligned} \text{TV}(u^{n+1}) &= \sum_j |u_j^{n+1} - u_{j-1}^{n+1}| = \\ &\leq \sum_j \left\{ \frac{\lambda}{4h} \Delta_{j+3/2} |u_{j+2} - u_{j+1}| + \frac{\lambda}{2} \varphi \Delta_{j+1/2} |u_{j+1} - u_j| \right. \\ &\quad \left. + \left( 1 - \lambda \left( \frac{1}{2h} + \varphi \right) \Delta_{j-1/2} \right) |u_j - u_{j-1}| \right. \\ &\quad \left. + \frac{\lambda}{2} \varphi \Delta_{j-3/2} |u_{j-1} - u_{j-2}| + \frac{\lambda}{4h} \Delta_{j-5/2} |u_{j-2} - u_{j-3}| \right\} \end{aligned} \quad (7)$$

provided that

$$(1 - \lambda \left( \frac{1}{2h} + \varphi \right) \Delta_{j-1/2}) \geq 0 \quad \forall j \quad (8)$$

Assuming that the data have compact support, we can rescale all sums and finally get  $\text{TV}(u^{n+1}) \leq \text{TV}(u^n)$ . Taking into account the Lipschitz condition on  $p$ , the scheme is total variation stable provided that (8) is satisfied, i.e. that

$$\Delta t \leq \frac{2h^2}{\mu} \frac{1}{1 + 2h\varphi} \simeq \frac{(2 - \delta)}{\mu} h^2 \quad (9)$$

where  $\delta$  vanishes as  $h$  does. We point out that the stability condition is of parabolic type. Finally, we observe that using one-sided approximations for the

partial derivatives of  $p$  in the scheme (6), one gets a stability condition involving the relation  $\varphi > 1/h$ . This would reintroduce in the scheme the constraint due to the stiffness in the convective term that prompted the introduction of  $\varphi$  in (3).

### 4.3 Linear stability

We study the linear stability of the schemes based on equations (3), (4) and (5) in the case when  $p(u) = u$ , by von Neumann analysis. We substitute the discrete Fourier modes  $u_j^n = \rho^n e^{i(jk/N)}$  into the scheme, where  $k$  is the wave number and  $N$  the number of cells. Let  $\xi = k/N$ , we compute the amplification factor  $Z(\xi)$  such that  $u_j^{n+1} = Z(\xi)u_j^n$ . We can consider  $\xi$  as a continuous variable, since the amplification factors for various choices of  $N$  all lie on the curves obtained considering the variable  $\xi \in [0, 2\pi]$ .

First we consider the same scheme studied in the previous section, for comparison purposes. Using piecewise constant reconstructions in space and forward Euler time integration, the amplification factor is  $Z(\xi) = 1 + M(\xi)$ , where

$$M(\xi) = \frac{\lambda}{h} (\cos(\xi) - 1) (\cos(\xi) + 1 + h\varphi).$$

$M(\xi)$  takes maximum value 0 and attains its minimum at the point  $\xi^*$  such that  $\cos(\xi^*) = -\varphi h/2$ . Stability requires that  $M(\xi^*) \geq -2$ , i.e.

$$1 + \frac{\lambda}{h} \left( \frac{\varphi^2 h^2}{4} - 1 \right) - \lambda \varphi \left( \frac{\varphi h}{2} + 1 \right) \geq -1$$

and recalling that  $\lambda = \Delta t/h$ ,

$$\Delta t \leq \frac{2h^2}{\left(1 + \frac{\varphi h}{2}\right)^2} \simeq 2(1 - \varphi h)h^2 \quad (10)$$

This gives a CFL condition of the form  $\Delta t \leq 2(1 - \delta)h^2$  where  $\delta = O(h\varphi)$  (see figure 1). These results are in very good agreement with those of the nonlinear analysis performed in the previous section.

Now we consider higher order spatial reconstructions coupled with forward Euler timestepping.  $M$  takes the form

$$M(\xi, \gamma) = \frac{\lambda}{h} [f_1(\cos(\xi)) + \gamma f_2(\cos(\xi))]$$

where  $\gamma = h\varphi$ . Since  $\gamma$  is small, we compute the critical points  $\xi^*$  of  $M(\xi, 0)$ . For stability we thus require that  $-2 \leq M(\xi^*, \gamma) \leq 0$ .

We consider a piecewise linear and a WENO reconstruction. The first one is computed along characteristic variables using the upwind slope, while the gradient of  $p(u)$  is computed with centered differences. The WENO reconstruction is fifth order accurate and is obtained by setting to 1 the smoothness indicators

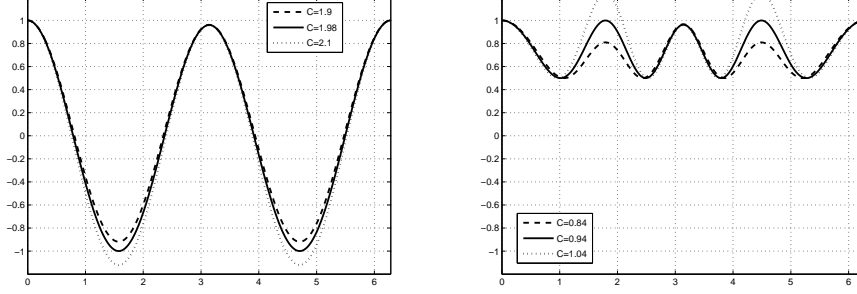


Figure 1: Amplification factor for upwind spatial reconstruction coupled with forward Euler (left) and for upwind second order spatial reconstruction coupled with second order time integration (right).

and the gradient of  $p(u)$  is computed with the fourth order centered difference formula.

For the piecewise linear reconstruction, we have that

$$M(\xi) = -\frac{\lambda}{h} [(\cos^2(\xi) - 1)(\cos(\xi) - 2) + h\varphi(\cos(\xi) - 1)^2] .$$

and therefore

$$\Delta t \leq \frac{2h^2}{\frac{20+14\sqrt{7}}{27} + \frac{8+2\sqrt{7}}{9}\varphi h} \simeq 0.94(1 - 1.44\varphi h)h^2$$

For the WENO reconstruction  $M(\xi, \gamma)$  can be easily computed and we get

$$\Delta t \leq 0.79(1 - 0.13\varphi h)h^2$$

Now we wish to extend our results to the case of higher order Runge-Kutta schemes. Since both the equation and the scheme are linear, the amplification factors for the Runge-Kutta schemes of order 2 and 3 used here are respectively

$$\begin{aligned} Z_{(2)}(\xi) &= 1 + M(\xi) + \frac{M(\xi)^2}{2} \\ Z_{(3)}(\xi) &= 1 + M(\xi) + \frac{M(\xi)^2}{2} + \frac{M(\xi)^3}{6} . \end{aligned}$$

where  $M(\xi)$  is the function appearing in the amplification factor relevant to the chosen spatial reconstruction. We have that

$$\begin{aligned} Z'_{(2)}(\xi) &= M'(\xi)(1 + M(\xi)) \\ Z'_{(3)}(\xi) &= M'(\xi)(1 + M(\xi) + \frac{M(\xi)^2}{2}) \end{aligned}$$

and therefore the critical points are the points  $\xi^*$  such that  $M'(\xi^*) = 0$ .



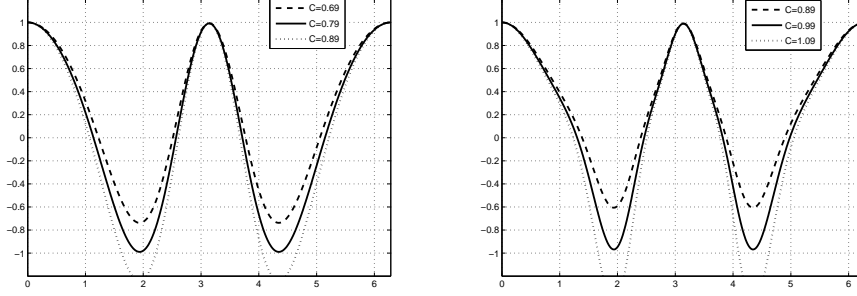


Figure 2: Amplification factors  $Z$  for WENO reconstructions of order 5 coupled with first order (left) and third order (right) time integration.

In the Runge-Kutta 2 case the stability constraint  $\|Z_{(2)}(\xi^*)\| \leq 1$  reduces to the CFL condition for the forward Euler scheme. For Runge-Kutta 3,  $\|Z_{(3)}(\xi^*)\| \leq 1$ , provided that

$$M(\xi^*) \geq \tilde{s} \simeq -2.51$$

Notice that this is less restrictive than the Euler and RK2 schemes for which the stability requirement is  $M(\xi^*) \geq -2$ .

For the Runge-Kutta 3 scheme with linearized WENO of order 5, we have

$$\Delta t \leq \frac{-\tilde{s}h^2}{2.51 + 0.33\varphi h} \simeq (1 - .1325\varphi h)h^2$$

Table 1 summarizes the stability results obtained in this section listing the values of the constant  $C$  that appear in the stability restriction  $\Delta t \leq C(1 - C_1\varphi h)h^2$ . Figures 1 and 2 contain the amplification factors  $Z(\xi)$  for  $\varphi = 1$  and  $h = 10^{-2}$  for various choices of spatial reconstructions and time integration schemes. Each of them contains the curve corresponding to the value of  $C$  reported in Table 1 and two other close-by values.

	RK1	RK2	RK3
P-wise constant	2	2	2.51
P-wise linear	0.94	0.94	
WENO5	0.79	0.79	1

Table 1:

#### 4.4 Boundary conditions

Different boundary conditions can be implemented. Here we describe how to implement Neumann boundary conditions, considering for simplicity the one-dimensional case.

We first add  $g$  ghost points on each side of the computational domain  $[a, b]$ , where  $g$  depends on the order of the spatial reconstruction. We find a polynomial  $q(x)$  of degree  $d$  passing through the points  $(x_i, u_i)$  for  $i = 1, \dots, d$  and having prescribed derivative at the boundary point  $x_{1/2} = a$ . (The degree  $d$  is determined by the accuracy of the scheme that one wants to obtain and should match the degree of the reconstruction procedures used to obtain  $U_j^\pm$  and  $V_j^\pm$ .) This polynomial is then used to set the values  $u_{-i} = q(x_{-i})$  of the ghost points for  $i = 0, 1, g-1$ . One operates similarly at the right edge of the computational domain.

We also used periodic boundary conditions, which can be implemented with obvious choice of the values  $u_i$  at the ghost points.

## 4.5 Multi-dimensional scheme

An appropriate numerical approximation of (3) in  $\mathbb{R}^d$  that generalizes the scheme described in Section 4.1 can be obtained by additive dimensional splitting. We consider the relaxed scheme, i.e.  $\varepsilon = 0$  and for the sake of simplicity, let us focus on the square domain  $[a, b] \times [a, b] \subset \mathbb{R}^2$ . Here we shall describe the generalization of the scheme defined by equations (3), (2), (4) and (5) to the case of two space dimensions.

Without loss of generality, we consider a uniform grid in  $[a, b] \times [a, b] \subset \mathbb{R}^2$  such that  $\vec{x}_{i,j} = (x_i, y_j) = (a - h/2, a - h/2) + i(h, 0) + j(0, h)$  for  $i, j = 1, 2, \dots, n$  and  $h = (b - a)/n$ .

In the present case,  $u$  and  $w$  are one-dimensional variables, while  $\vec{v} = (v_{(1)}, v_{(2)})$  is now a field in  $\mathbb{R}^2$ . First we observe that the relaxation steps (3) are easily generalized for  $d > 1$ . For the transport steps, one has to evolve in time the system

$$\frac{\partial}{\partial t} \begin{pmatrix} u \\ v_{(1)} \\ v_{(2)} \\ w \end{pmatrix} + \frac{\partial}{\partial x} \begin{bmatrix} 0 & 1 & 0 & 0 \\ 0 & 0 & 0 & \varphi^2 \\ 0 & 0 & 0 & 0 \\ 0 & 1 & 0 & 0 \end{bmatrix} \begin{pmatrix} u \\ v_{(1)} \\ v_{(2)} \\ w \end{pmatrix} + \frac{\partial}{\partial y} \begin{bmatrix} 0 & 0 & 1 & 0 \\ 0 & 0 & 0 & 0 \\ 0 & 0 & 0 & \varphi^2 \\ 0 & 0 & 1 & 0 \end{bmatrix} \begin{pmatrix} u \\ v_{(1)} \\ v_{(2)} \\ w \end{pmatrix} = 0 \quad (11)$$

The semidiscretization in space of the above equation can be written as

$$\frac{\partial z_{i,j}}{\partial t} = -\frac{1}{h} (F_{i+1/2,j} - F_{i-1/2,j}) - \frac{1}{h} (G_{i,j+1/2} - G_{i,j-1/2}),$$

where  $F$  and  $G$  are the numerical fluxes in the  $x$  and  $y$  direction respectively and can be written as

$$F_{i+1/2,j} = F(z_{i+1/2,j}^+, z_{i+1/2,j}^-) \quad G_{i,j+1/2} = G(z_{i,j+1/2}^+, z_{i,j+1/2}^-)$$

The fluxes in the two directions are computed separately. We illustrate the computation of the flux  $F$  along the  $x$  direction. We note that only the field  $v_{(1)}$  appears in the differential operator along this direction. The third component

of the flux is zero and thus we have three independent characteristic variables, namely

$$U_{(1)} = \frac{\varphi w + v_1}{2\varphi} \quad V_{(1)} = \frac{\varphi w - v_1}{2\varphi} \quad W = u - w,$$

which correspond respectively to the eigenvalues  $\varphi, -\varphi, 0$ . At this point the numerical fluxes can be easily evaluated by upwinding. We proceed similarly for the numerical flux  $G$  that depends on the characteristic variables  $U_{(2)}, V_{(2)}, W$ .

Denote by  $U_{i+1/2,j}^\pm$  the reconstructions of  $U_{(1)}(\cdot, y_j)$  at the point  $(x_i + h/2, y_j)$ . This involves a reconstruction of the restriction of  $U_{(1)}$  to the line  $y = y_j$  and can be obtained with any of the one-dimensional techniques mentioned in Section 4.1. Similarly, denote  $U_{i,j+1/2}^\pm$  the reconstructions of  $U_{(2)}(x_i, \cdot)$  at the point  $(x_i, y_j + h/2)$ . Now, formulas (4) and (5) become respectively

$$u_{i,j}^{(l)} = u_{i,j}^n - \lambda \sum_{m=1}^{l-1} \tilde{a}_{l,m} \left[ \varphi \left( U_{i+1/2,j}^{(m)-} - U_{i-1/2,j}^{(m)-} \right) - \varphi \left( V_{i+1/2,j}^{(m)+} - V_{i-1/2,j}^{(m)+} \right) \right. \\ \left. \varphi \left( U_{i,j+1/2}^{(m)-} - U_{i,j-1/2}^{(m)-} \right) - \varphi \left( V_{i,j+1/2}^{(m)+} - V_{i,j-1/2}^{(m)+} \right) \right] \quad (12)$$

and

$$u_{i,j}^{n+1} = u_{i,j}^n - \lambda \sum_{l=1}^{\nu} \varphi \tilde{b}_l \left[ \left( U_{i+1/2,j}^{(l)-} - V_{i+1/2,j}^{(l)+} \right) - \left( U_{i-1/2,j}^{(l)-} - V_{i-1/2,j}^{(l)+} \right) \right. \\ \left. \left( U_{i,j+1/2}^{(l)-} - V_{i,j+1/2}^{(l)+} \right) - \left( U_{i,j-1/2}^{(l)-} - V_{i,j-1/2}^{(l)+} \right) \right] \quad (13)$$

The generalization to  $d > 2$  and rectangular domains is now trivial. We stress once again that no two-dimensional reconstruction is used, but only  $d$  one-dimensional reconstructions are needed. Finally, boundary conditions can be implemented direction-wise with the same techniques used in the one-dimensional case.

## 5 Numerical results

We performed several numerical tests of our relaxed schemes. First we tested convergence for a linear diffusion equation with periodic and Neumann boundary conditions for initial data giving rise to smooth solutions. Next, numerical tests were also performed on the porous media equation  $u_t = (u^m)_{xx}$ ,  $m = 2, 3$ , both in one and two dimensions.

### 5.1 Linear diffusion

For the first test we considered the linear problem

$$\begin{cases} \frac{\partial u}{\partial t}(x, t) = \frac{\partial^2 u}{\partial x^2} u(x, t) & x \in [0, 1] \\ u(x, 0) = u_0(x) & x \in [0, 1] \end{cases}$$

First we used periodic boundary conditions with  $u_0(x) = \cos(2\pi x)$ , so that  $u(x, t) = \cos(2\pi x)e^{-4\pi^2 t}$  is an exact solution. Then we used Neumann boundary

	N=40	N=80	N=160	N=320	N=640
ENO2, RK1	2.012e-03	5.6378e-04	1.0736e-04	1.5539e-05	2.5065e-06
ENO3, RK2	1.9066e-06	2.3057e-07	5.6115e-08	8.6904e-09	1.1905e-09
ENO4, RK2	7.7517e-06	5.7082e-07	3.3507e-08	1.4978e-09	7.0725e-11
ENO5, RK3	1.3864e-08	6.0259e-10	2.2121e-11	7.4454e-13	2.3803e-14
ENO6, RK3	1.5538e-08	8.5661e-10	1.446e-11	1.7111e-13	1.5311e-15
WENO3, RK2	1.9799e-03	5.1278e-04	1.4332e-04	2.1488e-05	7.512e-08
WENO5, RK3	1.5892e-07	4.8069e-09	1.59e-10	5.2337e-12	1.6758e-13

	N=40	N=80	N=160	N=320	N=640
ENO2, RK1	1.3973	1.8354	2.3926	2.7886	2.6322
ENO3, RK2	5.9501	3.0477	2.0388	2.6909	2.8678
ENO4, RK2	3.8987	3.7634	4.0905	4.4836	4.4045
ENO5, RK3	6.8124	4.524	4.7677	4.8929	4.9671
ENO6, RK3	5.9907	4.181	5.8885	6.401	6.8043
WENO3, RK2	0.56648	1.949	1.8391	2.7376	8.1601
WENO5, RK3	2.9595	5.0471	4.918	4.925	4.9649

Table 1:  $L^1$  norms of the error and convergence rates for the linear diffusion equation with periodic boundary conditions, with smooth initial data

conditions  $u_x(0) = u_x(1) = 1$  with initial data  $u_0(x) = x + \cos(2\pi x)$ , so that  $u(x, t) = x + \cos(2\pi x)e^{-4\pi^2 t}$  is an exact solution.

We tested the numerical schemes defined by equations (2), (3), (4) and (5) with various degrees of accuracy for the spatial reconstructions and time-stepping operators. We used ENO spatial reconstructions of degrees from 2 to 6 and WENO reconstructions of degrees 3 and 5. The time-stepping procedures chosen are IMEX Runge-Kutta schemes of Section 3 of accuracy chosen to match the accuracy of the spatial reconstruction. Since stability forces the parabolic restriction  $\Delta t \leq Ch^2$ , an IMEX scheme of order  $m$  was coupled with a spatial ENO/WENO reconstruction of accuracy  $p$  such that  $p \leq 2m$ , obtaining a scheme of order  $p$ .

We computed the numerical solution of the diffusion equation with final time  $t = 0.05$  with  $N = 40, 80, 160, 320, 640$  grid points and computed the  $L^1$  norm of the difference between the numerical and the exact solution. The results are in Tables 1 for the periodic boundary conditions and 2 for the Neumann boundary conditions. One can see that the expected convergence rates are reached, even if the combination of the WENO reconstruction of accuracy 3 and the IMEX scheme of second order reach the predicted error reduction only on very fine grids.

## 5.2 Porous media equation

On the porous media equation (1) with  $p(u) = u^m$  we performed a test proposed in [16]. We took  $m = 2, 3$  and initial data of class  $C^1$  as follows:

$$u(x, 0) = \begin{cases} \cos^2(\pi x/2) & |x| \leq 1 \\ 0 & |x| > 1 \end{cases} \quad (1)$$

	N=40	N=80	N=160	N=320	N=640
ENO2, RK1	2.1965e-03	5.7152e-04	1.4301e-04	2.32e-05	4.743e-06
ENO3, RK2	2.0621e-06	2.2641e-07	6.7935e-08	8.8255e-09	1.2339e-09
ENO4, RK2	8.1764e-06	5.4431e-07	3.6974e-08	1.3686e-09	8.335e-11
ENO5, RK3	1.5484e-07	4.4163e-09	1.2405e-10	3.7803e-12	1.1669e-13
WENO3, RK2	1.9092e-03	4.4225e-04	1.2914e-04	4.5037e-06	7.4526e-08
WENO5, RK3	2.5048e-07	4.9279e-09	1.4776e-10	4.7482e-12	1.4948e-13

	N=40	N=80	N=160	N=320	N=640
ENO2, RK1	1.4361	1.9424	1.9987	2.624	2.2902
ENO3, RK2	6.1004	3.1871	1.7367	2.9444	2.8385
ENO4, RK2	3.9763	3.909	3.8798	4.7558	4.0373
ENO5, RK3	5.6626	5.1317	5.1539	5.0362	5.0178
WENO3, RK2	1.2624	2.11	1.7759	4.8417	5.9172
WENO5, RK3	4.9122	5.6676	5.0597	4.9597	4.9893

Table 2:  $L^1$  norms of the error and convergence rates for the linear diffusion equation with Neumann boundary conditions, with smooth initial data.

The computational domain is  $\{|x| \leq 3\} \subset \mathbb{R}$  and the boundary conditions are periodic; the CFL constant is taken as  $C = 0.25$ .

Since the initial data has compact support and is Lipschitz continuous, the solution will be of compact support for every  $t \geq 0$ , but will develop a discontinuity in  $u_x$  at some finite time  $\tau > 0$  (see [3]).

As was shown in [3], the solution with the initial condition we chose has a front that does not move for  $t < 0.034$ . We therefore chose a final time of the simulation  $t_{\text{fin}} = 0.03$  to prevent the formation of the singularity of  $u_x$  from affecting the order of convergence. We used as reference solution the one obtained numerically with  $N = 4860$  grid points and computed the  $L^1$  norms of the errors of the solutions with  $N = 60, 180, 540, 1620$  grid points. The results are presented in Table 3.

First of all one verifies that the degree of regularity of the solution poses a limit on the order of convergence of the schemes: therefore the schemes we tested perform at best as third order schemes, as confirmed by the data in Table 3. Still, high order schemes yield smaller error on a given grid. This can be of practical importance in problems where one does not have the freedom of choosing the number of grid points, as in digital image analysis, where non-linear degenerate diffusion equations are sometimes used as filters for contour enhancement (see [5]).

In Figure 1 we show the numerical solution for the porous media equation with  $p(u) = u^2$  and  $p(u) = u^3$ , with the initial data (1) and  $t \in [0, 2]$ . It can be appreciated that a front (i.e. a discontinuity of  $\frac{\partial u}{\partial x}$ ) develops at a finite time and then it travels at finite speed.

We present a numerical simulation for the two-dimensional porous media equation (1) with  $p(u) = u^2$ . We chose an initial data  $u_0(x, y)$  given by two bumps with periodic boundary conditions on  $[-10, 10] \times [-10, 10]$ . The large domain ensures that the compact support of the solution is still contained in the computational domain at the final time of the calculation. The numerical

	N=60	N=180	N=540	N=1620
ENO2, RK1	2.6365e-04	1.9898e-05	2.049e-06	2.076e-07
ENO3, RK2	1.9605e-05	6.0423e-07	2.4141e-08	8.9729e-10
ENO4, RK2	1.2127e-05	2.967e-07	9.9925e-09	3.5781e-10
ENO5, RK3	4.694e-06	1.719e-07	6.3248e-09	2.4447e-10
ENO6, RK3	4.1099e-06	1.4711e-07	5.3992e-09	2.0849e-10
WENO3, RK2	1.5871e-04	1.0448e-05	4.3463e-07	8.8767e-09
WENO5, RK3	7.5662e-06	4.6049e-07	7.4746e-09	2.7985e-10

	N=60	N=180	N=540	N=1620
ENO2, RK1	2.8243	2.352	2.0692	2.084
ENO3, RK2	5.1899	3.1672	2.931	2.9968
ENO4, RK2	5.6271	3.3774	3.0865	3.0307
ENO5, RK3	6.491	3.0103	3.006	2.9611
ENO6, RK3	6.612	3.0311	3.0083	2.962
WENO3, RK2	3.2863	2.4765	2.8942	3.5418
WENO5, RK3	6.0565	2.5479	3.7509	2.9902

Table 3:  $L^1$  norms of the error and convergence rates for the porous media equation periodic boundary conditions, with initial data of class  $C^1$ .

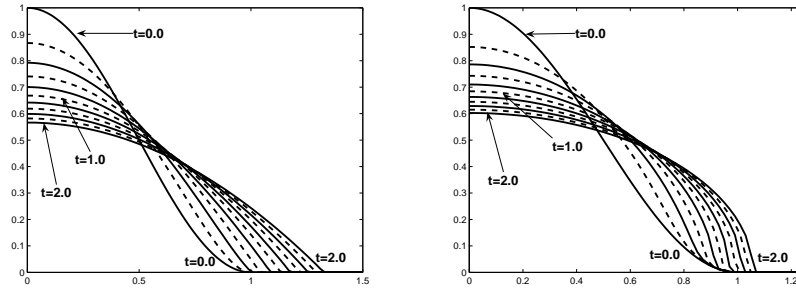


Figure 1: Snapshots of the numerical solutions for the porous media equation with  $p(u) = u^2$  (left) and  $p(u) = u^3$  (right). Initial data are chosen according to (1) and the numerical solutions are represented at times  $t = 0, 0.2, \dots, 2.0$ . The solutions are obtained with the spatial WENO reconstruction of order 5 and the RK3 time integrator.

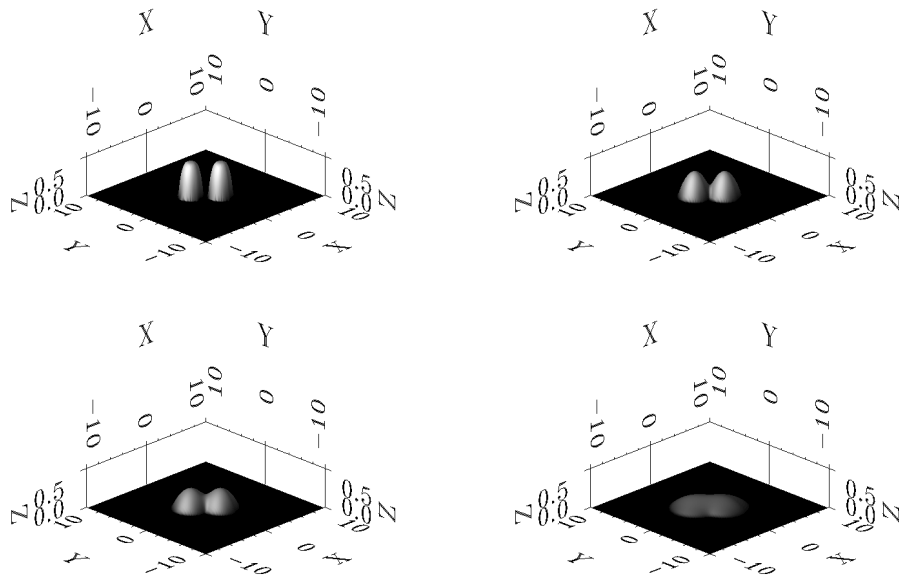


Figure 2: The numerical solution of the porous media equation on a square regular grid with compactly supported initial data. From top left to bottom right, we show the numerical solution at times  $t = 0, 0.5, 1.0, 4.0$ .

approximation at different time levels is shown in Figure 2.

We can note that the symmetries of the initial data are preserved and the solution seems to be unaffected by the dimensional splitting of the two-dimensional scheme.

## 6 Conclusions

We have proposed and analyzed relaxed schemes for nonlinear degenerate parabolic equations.

By using suitable discretization in space and time, namely ENO/WENO non-oscillatory reconstructions for numerical fluxes and IMEX Runge-Kutta schemes for time integration, we have obtained a class of high order schemes. We have developed a theoretical convergence analysis for the semidiscrete scheme; furthermore we studied stability for the fully discrete schemes. Our computational results suggest that our schemes converge with the predicted rate.

Finally, we point out that these schemes can be easily implemented on parallel computers. Some preliminary results and details are reported in [9]. In particular the schemes involve only linear matrix-vector operations and the execution time scales linearly when increasing the number of processors.

Our numerical approach can be easily extended also to more general problems, as nonlinear convection-diffusion equations or nonlinear parabolic systems. Some of these applications will appear in a forthcoming paper.

## References

- [1] D. AREGBA-DRIOLLET AND R. NATALINI, *Discrete kinetic schemes for multidimensional systems of conservation laws*, SIAM J. Numer. Anal., 37 (2000), pp. 1973–2004.
- [2] D. AREGBA-DRIOLLET, R. NATALINI, AND S. TANG, *Explicit diffusive kinetic schemes for nonlinear degenerate parabolic systems*, Math. Comp., 73 (2004), pp. 63–94.
- [3] D. G. ARONSON, *Regularity properties of flows through porous media: a counterexample.*, SIAM J. Appl. Math., 19 (1970), pp. 299–307.
- [4] U. ASHER, S. RUUTH, AND R.J. SPITERI, *Implicit-explicit Runge-Kutta methods for time dependent Partial Differential Equations*, Appl. Numer. Math., 25 (1997), pp. 151–167.
- [5] G. I. BARENBLATT AND J. L. VÁZQUEZ, *Nonlinear diffusion and image contour enhancement*, Interfaces Free Bound., 6 (2004), pp. 31–54.
- [6] A.E. BERGER, H. BREZIS, AND J.C.W. ROGERS, *A numerical method for solving the problem  $u_t - \Delta f(u) = 0$* , RAIRO numerical analysis, 13 (1979), pp. 297–312.



- [7] F. BOUCHUT, F. R. GUARGUAGLINI, AND R. NATALINI, *Diffusive BGK approximations for nonlinear multidimensional parabolic equations*, Indiana Univ. Math. J., 49 (2000), pp. 723–749.
- [8] H. BRÉZIS AND A. PAZY, *Convergence and approximation of semigroups of nonlinear operators in Banach spaces*, J. Functional Analysis, 9 (1972), pp. 63–74.
- [9] F. CAVALLI, G. NALDI, AND M. SEMPLICE, *Parallel algorithms for nonlinear diffusion by using relaxation approximation*, in ENUMATH 2005: Proceedings of the Conference held in Santiago de Compostela on July 18–22, 2005, Springer-Verlag, 2006. To appear.
- [10] F. COQUEL AND B. PERTHAME, *Relaxation of energy and approximate Riemann solvers for general pressure laws in fluid dynamics*, SIAM J. Numer. Anal., 35 (1998), pp. 2223–2249.
- [11] M.G. CRANDALL AND T.M. LIGGETT, *Generation of Semi-Groups of non linear transformations on general Banach spaces*, Amer. J. Math., 93 (1971), pp. 265–298.
- [12] MAGNE S. ESPEDAL AND KENNETH HVISTENDAHL KARLSEN, *Numerical solution of reservoir flow models based on large time step operator splitting algorithms*, in Filtration in porous media and industrial application (Cetraro, 1998), vol. 1734 of Lecture Notes in Math., Springer, Berlin, 2000, pp. 9–77.
- [13] S. EVJE AND K. H. KARLSEN, *Viscous splitting approximation of mixed hyperbolic-parabolic convection-diffusion equations*, Numer. Math., 83 (1999), pp. 107–137.
- [14] A. FRIEDMAN, *Mildly nonlinear parabolic equations with application to flow gases through porous media*, Arch. Rational Mech. Anal., 5 (1960), pp. 238–248 (1960).
- [15] S. GOTTLIEB, C. SHU, AND E. TADMOR, *Strong stability-preserving high-order time discretization methods*, SIAM Rev., 43 (2001), pp. 89–112.
- [16] J. L. GRAVELEAU AND P. JAMET, *A finite difference approach to some degenerate nonlinear parabolic equations*, SIAM J. Appl. Math., 20 (1971), pp. 199–223.
- [17] W. JÄGER AND J. KAVCUR, *Solution of porous medium type systems by linear approximation schemes*, Numer. Math., 60 (1991), pp. 407–427.
- [18] S. JIN, *Runge-Kutta methods for hyperbolic conservation laws with stiff relaxation terms*, J. Comput. Phys., 122 (1995), pp. 51–67.
- [19] S. JIN, M. A. KATSOULAKIS, AND Z. XIN, *Relaxation schemes for curvature-dependent front propagation*, Comm. Pure Appl. Math., 52 (1999), pp. 1587–1615.

- [20] S. JIN AND C. D. LEVERMORE, *Numerical schemes for hyperbolic conservation laws with stiff relaxation terms*, J. Comput. Phys., 126 (1996), pp. 449–467.
- [21] S. JIN, L. PARESCHI, AND G. TOSCANI, *Diffusive relaxation schemes for multiscale discrete velocity kinetic equations*, SIAM J. Numer. Anal., 35 (1998), pp. 2405–2439.
- [22] S. JIN AND M. SLEMROD, *Regularization of the Burnett equations for rapid granular flows via relaxation*, Phys. D, 150 (2001), pp. 207–218.
- [23] S. JIN AND Z. XIN, *The relaxation schemes for systems of conservation laws in arbitrary space dimension*, Comm. Pure and Appl. Math., 48 (1995), pp. 235–276.
- [24] J. KAČUR, A. HANDLOVIČOVÁ, AND M. KAČUROVÁ, *Solution of nonlinear diffusion problems by linear approximation schemes*, SIAM J. Numer. Anal., 30 (1993), pp. 1703–1722.
- [25] P.L. LIONS AND G. TOSCANI, *Diffusive limit for two-velocity Boltzmann kinetic models*, Rev. Mat. Iberoamericana, 13 (1997), pp. 473–513.
- [26] E. MAGENES, R. H. NOCHETTO, AND C. VERDI, *Energy error estimates for a linear scheme to approximate nonlinear parabolic problems*, RAIRO Modél. Math. Anal. Numér., 21 (1987), pp. 655–678.
- [27] G. NALDI AND L. PARESCHI, *Numerical schemes for hyperbolic systems of conservation laws with stiff diffusive relaxation*, SIAM J. Numer. Anal., 37 (2000), pp. 1246–1270.
- [28] G. NALDI, L. PARESCHI, AND G. TOSCANI, *Relaxation schemes for partial differential equations and applications to degenerate diffusion problems*, Surveys Math. Indust., 10 (2002), pp. 315–343.
- [29] R. H. NOCHETTO, A. SCHMIDT, AND C. VERDI, *A posteriori error estimation and adaptivity for degenerate parabolic problems*, Math. Comp., 69 (2000), pp. 1–24.
- [30] R. H. NOCHETTO AND C. VERDI, *Approximation of degenerate parabolic problems using numerical integration*, SIAM J. Numer. Anal., 25 (1988), pp. 784–814.
- [31] L. PARESCHI AND G. RUSSO, *Implicit-explicit Runge-Kutta schemes and applications to hyperbolic systems with relaxation*, J. Sci. Comp., 25 (2005), pp. 129–155.
- [32] I. S. POP AND W. YONG, *A numerical approach to degenerate parabolic equations*, Numer. Math., 92 (2002), pp. 357–381.

- [33] C. SHU, *Essentially non-oscillatory and weighted essentially non-oscillatory schemes for hyperbolic conservation laws*, in Advanced numerical approximation of nonlinear hyperbolic equations (Cetraro, 1997), vol. 1697 of Lecture Notes in Math., Springer, Berlin, 1998, pp. 325–432.
- [34] C. SHU AND S. OSHER, *Efficient implementation of essentially nonoscillatory shock-capturing schemes. II*, J. Comput. Phys., 83 (1989), pp. 32–78.
- [35] J. L. VÁZQUEZ, *An introduction to the mathematical theory of the porous medium equation*, in Shape optimization and free boundaries (Montreal, PQ, 1990), vol. 380 of NATO Adv. Sci. Inst. Ser. C Math. Phys. Sci., Kluwer Acad. Publ., Dordrecht, 1992, pp. 347–389.
- [36] J. WEICKERT, *Anisotropic diffusion in image processing*, European Consortium for Mathematics in Industry, B. G. Teubner, Stuttgart, 1998.